



CHORUS

This is the accepted manuscript made available via CHORUS. The article has been published as:

Characterization of thermal transport in low-dimensional boron nitride nanostructures

Cem Sevik, Alper Kinaci, Justin B. Haskins, and Tahir Çağın

Phys. Rev. B **84**, 085409 — Published 22 August 2011

DOI: [10.1103/PhysRevB.84.085409](https://doi.org/10.1103/PhysRevB.84.085409)

Characterization of Thermal Transport in Low-Dimensional Boron Nitride Nanostructures

Cem Sevik,^{1,2,*} Alper Kinaci,² Justin B. Haskins,¹ and Tahir Çağın^{1,2,†}

¹*Artie McFerrin Department of Chemical Engineering,
Texas A&M University, College Station, TX 77845-3122, USA*

²*Material Science and Engineering, Texas A&M University,
College Station, TX 77845-3122, USA*

Abstract

Recent advances in the synthesis of hexagonal boron nitride (BN) based nanostructures, similar to graphene, graphene nanoribbons, and nanotubes, have attracted significant interest into characterization of these materials. While electronic and optical properties of BN based materials have been widely studied, the thermal transport has not been thoroughly investigated. In this paper, the thermal transport properties of these BN nanostructures are systematically studied using equilibrium molecular dynamics with a Tersoff type empirical interatomic potential which is reparameterized to represent experimental structure and phonon dispersion of 2D hexagonal BN. Our simulations show that BN nanostructures have considerably high thermal conductivities but are still quite lower than carbon based counterparts. Qualitatively, however, the thermal conductivity of carbon and BN nanoribbons display similar behavior with respect to the variation of width and edge structure (zigzag and armchair). Additionally, thermal conductivities of (10,10) and (10,0) nanotubes, both carbon and BN, are found to have very weak dependence on their chirality.

PACS numbers: 61.46.-w, 65.80.+n, 68.65.-k, 66.70.-f

I. INTRODUCTION

Advances in nanoscale synthesis and processing going beyond carbon based chemistries have lead to new and novel opportunities. The increasing control on dimension and length scale raises hope to control and tune the physical properties of various materials in lower dimensions and nanometer scales for new technological applications. For instance, carbon based nanomaterials, in particular, buckyballs, nanotubes, graphene sheets and graphene ribbons have been extensively studied and repeatedly reported as promising candidates for next generation electronics¹⁻⁸. The encouraging performance of carbon based honeycomb structures has stimulated strong interest in isomorphous materials based on Boron Nitride (BN)⁹⁻²². Their outstanding physical properties, superb thermal and chemical stability²³, and intrinsic electrical insulation^{24,25}, along with the independence of these properties from the chirality, diameter and wall-wall interactions in tubes and the width in ribbons^{26,27} have put these nanomaterials at the forefront of current nanoscience research.

Most of the experimental and theoretical studies focus on the mechanical²⁸, electrical²⁹⁻³³ and optical properties³⁴⁻³⁸ of these materials, as well as some uncommon physical phenomena such as inducible magnetization³⁹ in two dimensional hexagonal BN (white graphene) with defect engineering^{40,41}, correlated motifs observed in multi-wall BN nanotubes (BNNTs)⁴², and peculiar emergence of substantial charge density inside the tube rather than on the tube upon electron doping of BNNTs¹³. Unlike carbon, limited work has been published on the thermal transport properties⁴³⁻⁴⁹ of BN nanostructures despite their potential use in nanoscale thermal management applications due to their remarkable thermal transport properties comparable to carbon based nanostructures⁵⁰⁻⁶³.

The first principles calculations of thermal transport properties of nanostructures such as nanoribbons require prohibitively large and complex model structures. The calculations are usually performed with very narrow widths, which might lead to unreliable results due the strong width dependence. Furthermore, determination of the relaxation time(s) requires higher order derivatives to be evaluated from a first principles calculation in Boltzmann Transport Equation (BTE) approach. On the other hand, classical equilibrium molecular dynamic (MD) simulations with Green-Kubo theory presents a viable and very successful approach, especially for determination of lattice thermal conductivity as a function of dimensionality and length scales relevant to realistic nanostructured materials. The interaction

potential is the key for accurate results in MD studies. For thermal transport, the main requirement is to have an interaction potential particularly reproducing the phonon spectra and associated group velocities in agreement with the experiment and first principles theory. To the best of our knowledge there is no reliable potential satisfying this criteria.

For this study, as a first step, we develop a Tersoff type interaction potential parameter set (IPP) with particular attention to reproduce structural, mechanical, and vibrational properties of hexagonal BN. Then using this IPP set, the lattice thermal conductivity values of the BN based nanostructures shown in Fig. 1: white graphene (BNWG), BNNTs with zigzag (10,0) and armchair (10,10) chirality, and white graphene ribbons having zigzag and armchair edge structures, (z-BNNR and a-BNNR), were systematically determined using equilibrium MD simulations at various temperatures through Green-Kubo formalism. This method has been successfully used in many systems^{64–67}. Here, in order to present a comparative analysis, computations were also performed for the equivalent carbon based nanostructures (exactly the same method and structures) using again an accurate Tersoff type IPP set for carbon⁶⁸.

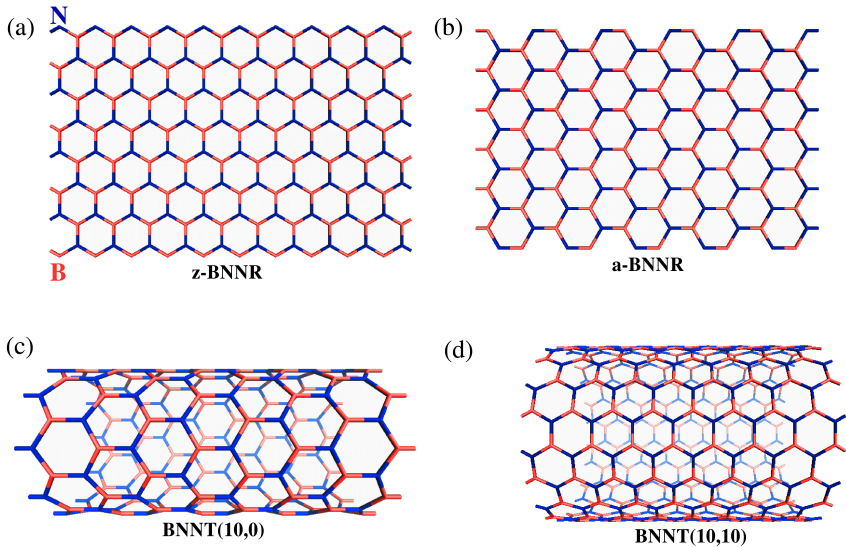


FIG. 1: (Color online) Schematic description of BN nanostructures, (a) zigzag BN nanoribbon (z-BNNR), (b) armchair BN nanoribbon (a-BNNR), (c) (10,0) BN nanotube (BNNT), and (d) (10,10) BN nanotube.

II. METHODS

The transport coefficients can be calculated through MD by using the Green-Kubo relations derived from the fluctuation dissipation theorem⁶⁹⁻⁷¹ and equivalently by an expression akin to the Einstein diffusion relationships⁷²⁻⁷⁴. For the lattice thermal conductivity, κ , the Einstein relation can be written as

$$\kappa_{\mu\mu} = \frac{1}{Vk_B T^2} \lim_{t \rightarrow \infty} \frac{1}{2t} \langle [R_\mu(t) - R_\mu(0)]^2 \rangle \quad (1)$$

where, T , V , and k_B are the temperature, volume, Boltzmann constant, respectively and R_μ is the time integration of heat current in direction μ . Ordinarily, R_μ for a single particle is the total energy of the particle, ϵ_i , times its unwrapped coordinate, $r_{i\mu}$, in the simulation domain. The total R_μ of the system is calculated by a summation over all particle as given in Eq. 2.

$$R_\mu = \sum_i r_{i\mu} \epsilon_i, \quad (2)$$

that can be thought of as energy moment vector for the system. In application to molecular dynamics, discrepancies arise regarding the equivalence of the Einstein relation and the Green-Kubo approach⁷⁵; nevertheless it is still possible to write an explicit functional form for R_μ ^{76,77}.

Molecular dynamics simulations in micro canonical ensemble are performed with a time step of 1 fs that reliably converges R_μ . The systems first relaxed for 250 ps. Then, each thermal conductivity data point is obtained from the average of six such simulations, all lasting a minimum of 5 ns. In the case of the κ calculations, the slope, defined by the time limit in Eq. 1, is obtained by fitting the diffusion like term to a linear function i.e. $y = slope \times t$. Moreover, $\pi[(r + \frac{\Delta}{2})^2 - (r - \frac{\Delta}{2})^2]$ and $(w \times \Delta)$ are used as cross-sectional areas of the tube and ribbon structures, respectively, where r is the BNNT radius, w is the ribbon width and Δ , 0.335 nm, is the mean Van der Waals diameter for (B and N atoms) of hexagonal boron nitride.

The form Tersoff IPP⁷⁸ used in this study can be written as

$$\begin{aligned}
V_{ij} &= f_C(r_{ij}) [f_R(r_{ij}) + b_{ij}f_A(r_{ij})] \\
f_C(r) &= \begin{cases} 1 & : r < R - D \\ \frac{1}{2} - \frac{1}{2} \sin\left(\frac{\pi}{2} \frac{r-R}{D}\right) & : R - D < r < R + D \\ 0 & : r > R + D \end{cases} \\
f_R(r) &= A \exp(-\lambda_1 r) \\
f_A(r) &= -B \exp(-\lambda_2 r) \\
b_{ij} &= (1 + \beta^n \zeta_{ij}^n)^{-\frac{1}{2n}} \\
\zeta_{ij} &= \sum_{k \neq i, j} f_C(r_{ik}) g(\theta_{ijk}) \exp[\lambda_3^3 (r_{ij} - r_{ik})^3] \\
g(\theta) &= \left(1 + \frac{c^2}{d^2} - \frac{c^2}{[d^2 + (\cos \theta - h)^2]}\right) \tag{3}
\end{aligned}$$

where f_R is a two-body term, f_A includes three-body interactions and f_C is a cutoff term to guarantee first nearest-neighbor interaction. b_{ij} is the bond angle term which depends on the local coordination of atoms around atom i and the angle between atoms i , j , and k (θ_{ijk}). The summation in the formula are over all neighbors j and k of atom i within a cutoff distance equal to $R + D$.

First principles calculations were performed with Vienna *ab initio* simulation package (VASP)^{79,80} which is based on density functional theory⁸¹. Projector augmented wave^{82,83} pseudo potential formalism was imposed together with local density (LDA) and Perdew-Burke-Ernzerhof (PBE)⁸⁴ form of generalized gradient approximations (GGA). In the case of the calculations for BNWG (BNNTs) 500 eV plane wave energy cut-off and $24 \times 24 \times 1$ ($1 \times 1 \times 12$) Monkhorst-Pack k point grid were used in order to achieve required energy convergence. Phonon dispersion relations were determined by using *ab initio* force constant method as described in Parlinski *et al.*⁸⁵.

III. RESULTS AND DISCUSSIONS

1. New Tersoff interaction potential parameters for BN

In order to accurately determine the lattice thermal conductivity of a material with molecular dynamic simulations, it is critical that the IPP set produces an accurate acoustic phonon

dispersion and corresponding group velocities⁸⁶. With this objective in mind, we first fitted a Tersoff type IPP set, listed in Table I, to structural, mechanical and dynamical properties of hexagonal BN nanostructures. The resulting parameter set produces highly consistent results when compared to both first principles and experimental data. For instance, the variation of total energies of BNWG with unit cell area and the variation of total energies of BNNTs with lattice constant along the nanotube axes, c , (ions are fully relaxed for each c), shown in Fig. 2, have very good agreement with first-principles calculations performed using both LDA and GGA. The calculated equilibrium lattice constant of hexagonal BN, a_0 , 2.498 Å, closely matches to the experimental value, 2.500 Å^{15,18}. Furthermore, the radial strain energy (strain energy per atom: $E_{BNNT} - E_{BNWG}$) shows a close agreement with the first-principles calculations⁸⁷.

TABLE I: Tersoff type optimized interatomic potential parameters for hexagonal Boron Nitride structures. These parameters are valid for all atoms interacting within first neighbor range as depicted by this Tersoff potential shown in methods section.

A (eV)	1380	B (eV)	340.0
λ_1 (Å ⁻¹)	3.568	λ_2 (Å ⁻¹)	2.199
λ_3 (Å ⁻¹)	0.000	n	0.72751
c	25000	β (10 ⁻⁷)	1.25724
d	4.3484	h	-0.89000
R (Å)	1.950	D (Å)	0.050

The calculated vibrational properties of BNWG, especially longitudinal, transverse, and out-of-plane acoustic branches (LA, TA and ZA), have excellent agreement with both first-principles and experimental⁸⁸ results, as seen in Fig. 3. Even though the out-of-plane optical (ZO) branch slightly deviates from the standard at Γ and K , the rest of the calculated frequencies for this mode along the high symmetry directions match the experimental values. To note the only weakness of the IPP in describing the vibrational properties is in the longitudinal and transverse optical branches (LO and TO). However, the effect of these phonons on lattice thermal conductivity is less important due to their very low phonon group velocities.

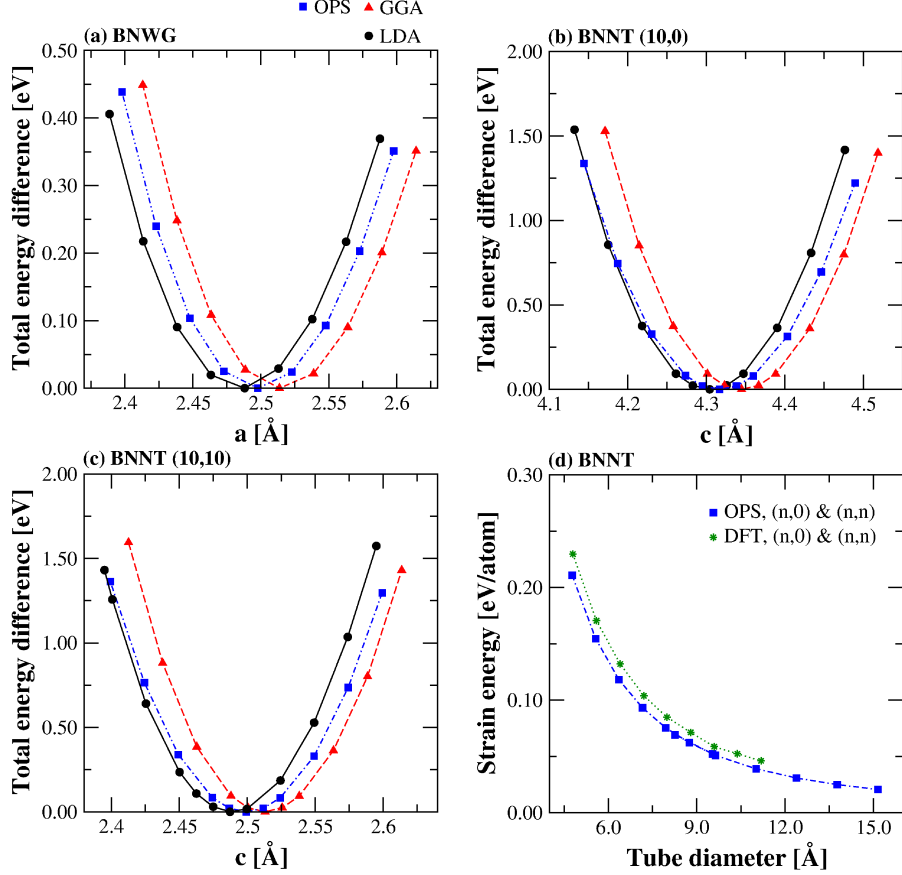


FIG. 2: (Color online) (a) Variation of total energy of BNWG with lattice constant, a . Variation of total energy of (b) (10,0) and (c) (10,10) BNNT with lattice constant along the tube axes, c . (d) Strain energy versus BNNT diameter. Here, the data specified by OPS and LDA (GGA) represent our results obtained with optimized Tersoff parameter set and first principles LDA (GGA) approximation, and DFT represents the data taken from Ref. 87.

2. Boron Nitride Nanostructures

Using the corresponding “Einstein Equation” (see Methods section), the temperature dependent lattice thermal conductivities of BNWG, BNNRs and BNNTs were calculated. For all systems, the reported thermal conductivity, κ , values were obtained from the average of six independent MD simulations (with different initial conditions, namely different Maxwell-Boltzmann velocity distributions at the same temperature); and the standard error bars are calculated from the standard deviation of these six equivalent but independent runs. Fig. 4 shows the variation of κ , in periodic armchair and zigzag directions, with temperature for

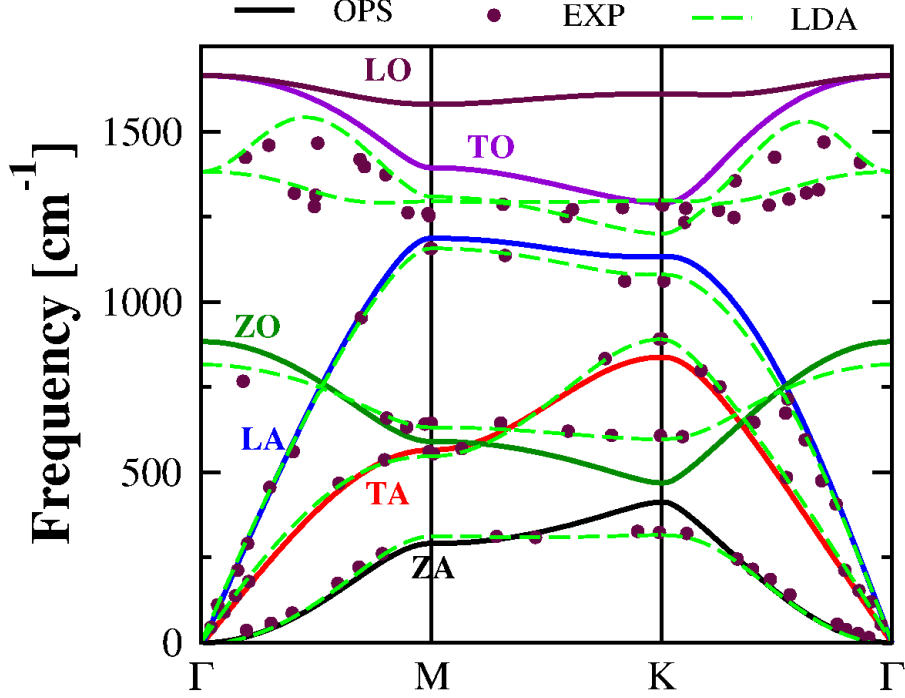


FIG. 3: (Color online) Phonon dispersion of BNWG along the high symmetry reciprocal space points (solid lines) and comparison with first principles (dashed lines) and experimental (dotted, Ref. 88) results.

BNWG modeled in a 40 nm×40 nm rectangular periodic simulation box. The box length in z -direction is chosen considerably larger than the cut off length so that there is no interaction between periodic images in z -direction. Our results for κ of BN based materials are comparable with high thermal conductivity metals. Still, these values cannot reach to the thermal conductivity values of similar carbon based structures. For instance, the room temperature thermal conductivity of BNWG is approximately six times smaller than the one obtained for graphene, see in Table II.

From the kinetic theory, it is well known that the thermal conductivity is related to specific heat, phonon group velocities and phonon mean-free path. Therefore, further calculations were done in order to clarify the effect of specific heat, group velocities and mass difference on the κ of graphene and BNWG. First, the specific heats of graphene and BNWG were calculated from energy fluctuations in MD^{72,89}. They are nearly the same in 2%. However, the group velocities, $\frac{dw(q)}{dq}$, of acoustic phonon branches of BNWG, are much lower than that of graphene. See Fig. 5 (a) and (b) for OPS and LDA calculations. As a consequence, the

faster phonon modes of graphene, around Brillouin zone center Γ point, can be considered as one of the main reason of the observed difference in κ , between GNR and BNWG, due to their quadratic contribution to κ ⁹⁰. Different masses of B and N would also be expected to decrease thermal conductivity by introducing additional mechanism for phonon scattering⁶⁴. To demonstrate this effect, two artificial model systems are generated, “graphene” in which carbon-carbon interactions are defined as boron-nitrogen interactions in our potential and a “BNWG” in which boron-nitrogen interactions are defined as carbon-carbon interactions in Tersoff carbon potential⁶⁸. First, we applied lattice dynamics to the model “graphene”, and model “BNWG”, to compare with the phonon spectra and phonon group velocities of the original ones. We obtained similar phonon group velocities for model “graphene” (“BNWG”) and original BNWG (graphene). Furthermore, to see the resulting effect on κ , MD simulations also performed for these model “graphene” and “BNWG” at room temperature. The resulting κ of the model “graphene” system is $\sim 20\%$ larger than that of BNWG. On the other hand, the κ of model “BNWG” is $\sim 20\%$ smaller than that of graphene. This supports the statement made above on the mass difference leading to reduction in κ . To quantitatively assess the influence of mean-free paths for BN and graphene requires additional calculations^{91,92} using higher order derivatives of potential energy surface, which are out of the scope of the current study.

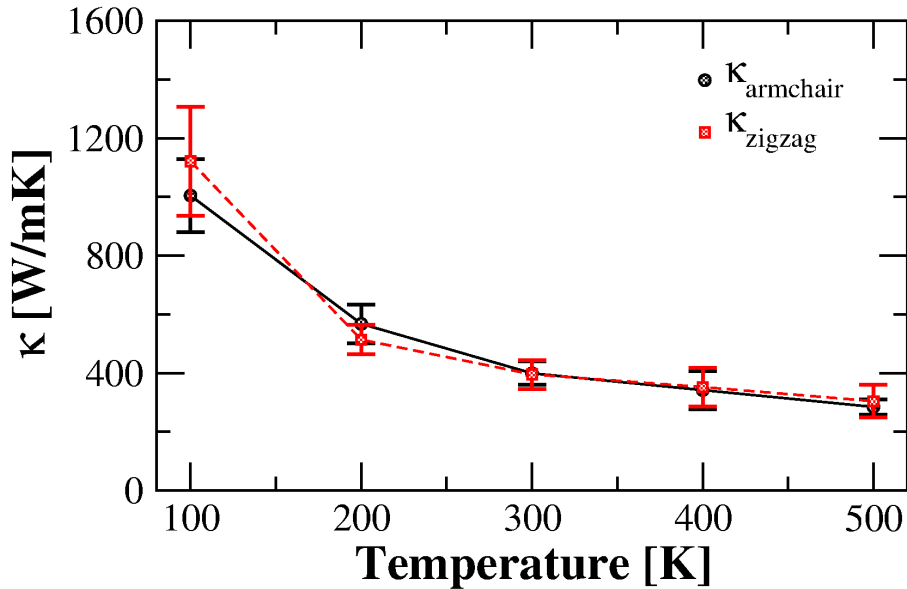


FIG. 4: (Color online) Temperature dependence of lattice thermal conductivities of BNWG through armchair and zigzag directions.

TABLE II: The room temperature lattice thermal conductivity values for BN nanostructures and their exact carbon conjugates calculated from MD simulations. The results for graphene and GNRs are taken from Ref. 93

Structure	κ [W/mK]	Structure	κ [W/mK]
Graphene	2500	BNWG	400
z-GNR(~ 12 nm)	1700	z-BNNR(~ 12 nm)	350
z-GNR(~ 20 nm)	2300	z-BNNR(~ 20 nm)	380
a-GNR(~ 12 nm)	1025	a-BNNR(~ 12 nm)	260
a-GNR(~ 20 nm)	1859	a-BNNR(~ 20 nm)	360
CNT(10,0)	955	BNNT(10,0)	430
CNT(10,10)	940	BNNT(10,10)	465

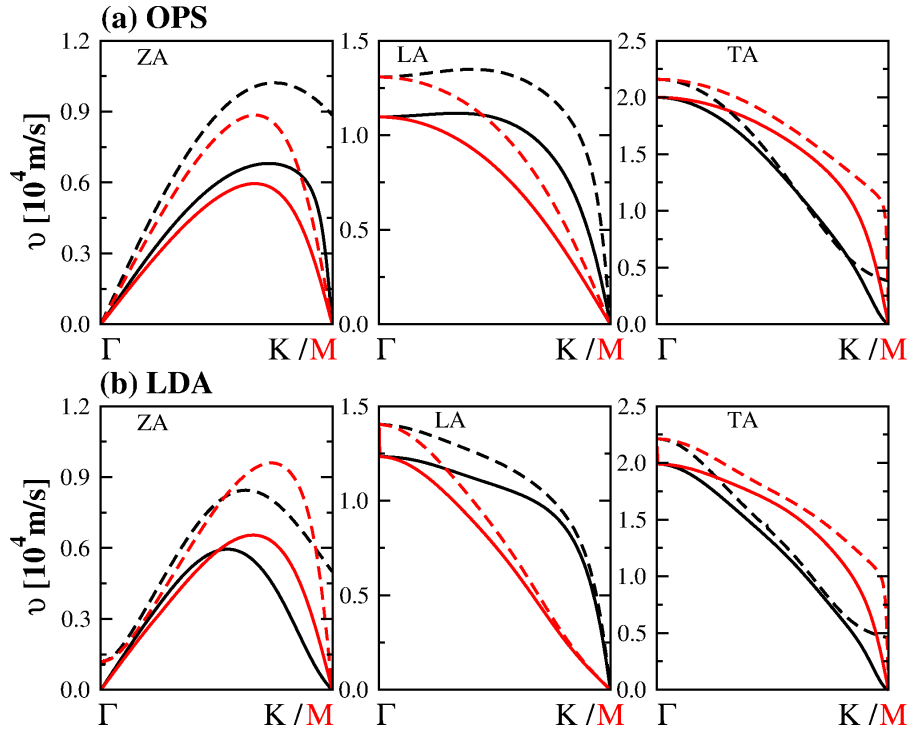


FIG. 5: (Color online) Phonon group velocity of BNWG and its carbon based isomorph, graphene, along Γ to K (black lines) and Γ to M (red lines) directions. Here, solid and dashed lines represents BNWG and graphene, respectively.

The effects of the width and edge structure on lattice thermal conductivity of BNWG were also investigated by considering both zigzag and armchair nanoribbon structures with

varying widths, see Fig. 6 (a). Here, lengths of the structures were chosen around 250 nm in order to avoid artificial phonon scattering due to the phonons re-entering the periodic simulations box without getting dissipated⁹³. In the case of the nanoribbon simulations, the mass of edge atoms were increased by 1 amu to imitate hydrogen termination⁹⁴. Our results show that the ribbon width has strong influence on lattice thermal conductivity of both z-BNNRs and a-BNNRs, similar to the previously reported graphene nanoribbon results⁹³, as depicted in Fig. 6. At a width value of 2.5 nm, the κ of z-BNNRs is considerably greater than that of a-BNNRs. As the width increases, however, the κ of both edge forms of BNNR steadily converge with z-BNNRs remaining slightly higher at 20 nm. These observations are related to the higher number of edge scatterers in a-BNNRs compared to z-BNNRs on a unit length basis, a significant effect especially for narrow nanoribbons⁹³. The conductivity of z- and a-BNNRs are four or six times smaller than that of graphene nanoribbons as listed in Table II. However, the overall qualitative effect of edges is the same for both nanosystems. Previous studies^{43,95} on BNNR's using non-equilibrium Green's functions method give much higher results, 1700-3000 W/mK, for thermal conductivity. This difference with MD could be emanating from the ballistic nature of Green's functions calculations. In the case of classical MD method the strong phonon scattering restrict such high values of κ .

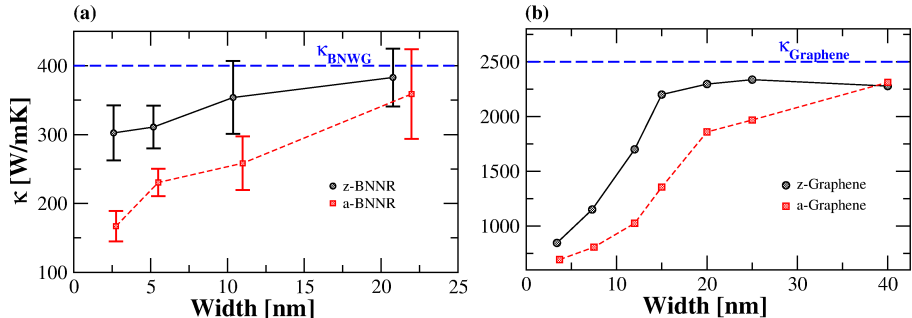


FIG. 6: (Color online) The width dependence of room temperature lattice thermal conductivity in a- and z- (a) BNNRs and (b) GNRs. The GNR results are adopted from Ref. 93.

Finally, two different types of BNNTs, zigzag and armchair, with 200 nm length were systematically investigated by simulating in rectangular periodic simulation boxes. As seen in Fig. 7, BNNTs have a chirality insensitive thermal conductivity as previously published for CNTs⁹⁶⁻⁹⁸ which ranges from 400-450 W/mK at room temperature. Like the other BN nanostructures, the thermal conductivities, while remarkably large, are still 50% less

than that of CNTs. Whereas CNTs have significantly lower thermal conductivities when compared to graphene, BNNTs and BNWG have similar values of thermal conductivity, Table II. The difference between carbon and BN nanostructures, predicted for all systems considered in this study, might again be attributed to the lower group velocities²⁸ and different mass fluctuations of BN nanostructures.

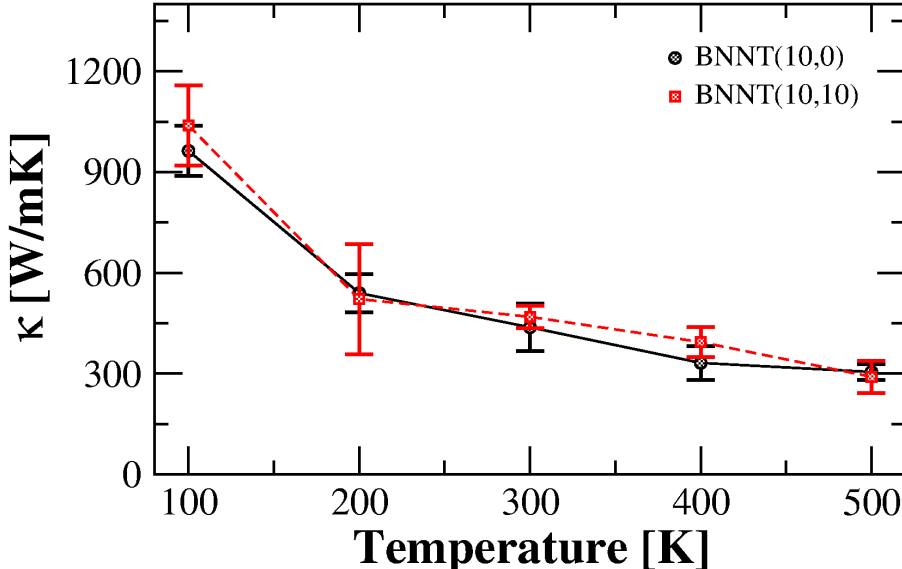


FIG. 7: (Color online) Temperature dependence of lattice thermal conductivities of BNNTs with two different chiralities, (10,0) and (10,10).

IV. SUMMARY AND CONCLUDING REMARKS

In summary, we presented a detailed investigation of lattice thermal conductivity of Boron Nitride based nanomaterials using molecular level theories. For this purpose, we developed a new Tersoff type interaction potential parameter set that effectively represent the experimental phonon dispersion for BN. Furthermore, in order to make a clear comparison between BN and carbon based materials, lattice thermal conductivities of equivalent carbon based nanostructures were also calculated. The predicted thermal conductivities of BNNTs and BNWG are on the order of common high thermal conductivity bulk materials, excluding diamond. However, all the BN based nanomaterials considered in this study have lower thermal conductivity than their carbon analogues. We identified two possible reasons for this disparity. First is the softer phonon modes, especially in the acoustic branches of BN

based systems. Second is the mass difference of B and N. Despite this quantitative difference, qualitative aspects are very similar in BN and carbon structures. Both CNTs and BNNTs exhibit thermal conductivities independent of considered chiralities. Moreover, as a function of width, the thermal conductivity of GNR and BNNRs follow similar trends with respect to two different edge structures. The only significant difference is in how the thermal conductivity varies between planar and tubular topology in the same chemistry; graphene has higher κ than CNT while BNWG has nearly the same κ with BNNT.

V. ACKNOWLEDGEMENTS

We acknowledge the support from NSF (DMR 0844082) to International Institute of Materials for Energy Conversion at Texas A&M University as well as AFRL. The parts of computations are carried out at the facilities of Laboratory of Computational Engineering of Nanomaterials also supported by ARO, ONR and DOE grants. We also would like to thank for generous time allocation made for this project by the Supercomputing Center of Texas A&M University.

* Electronic address: sevik@tamu.edu

† Electronic address: tcagin@tamu.edu

¹ S. Iijima, *Nature* **354**, 56 (1991).

² R. Saito, G. Dresselhaus, and M. S. Dresselhaus, *Physical Properties of Carbon Nanotubes* (Imperial College Press, London, 1998).

³ R. Saito, G. Dresselhaus, and M. S. Dresselhaus, *Carbon Nanotubes: Synthesis, Structure, Properties, and Applications* (Springer-Verlag, Berlin, 2001).

⁴ A. H. Castro Neto, F. Guinea, N. M. R. Peres, K. S. Novoselov, and A. K. Geim, *Rev. Mod. Phys.* **81**, 109 (2009).

⁵ K. Wakabayashi, Y. Takane, and M. Sgrist, *Phys. Rev. Lett.* **99**, 036601 (2007).

⁶ Y. Zhang, Y. Tan, H. Stormer, and P. Kim, *Nature* **438**, 201 (2005).

⁷ J. Che, T. Çağın, and W. Goddard III, *Nanotechnology* **11**, 65 (2000).

⁸ J. Lukes and H. Zhong, *J. Heat Transf.* **129**, 705 (2007).

- ⁹ C. Zhi, Y. Bando, C. Tang, and D. Golberg, *Mater. Sci. Eng. R.* **70**, 92 (2010).
- ¹⁰ R. S. Lee, J. Gavillet, M. L. d. l. Chapelle, A. Loiseau, J.-L. Cochon, D. Pigache, J. Thibault, and F. Willaime, *Phys. Rev. B* **64**, 121405 (2001).
- ¹¹ C. Y. Zhi, Y. Bando, C. C. Tang, Q. Huang, and D. Golberg, *J. Mater. Chem.* **18**, 3900 (2008).
- ¹² N. G. NG Chopra, R. J. Luyken, K. Cherrey, V. H. Crespi, M. L. Cohen, S. G. Louie, and A. Zettl, *Science* **269**, 966 (1995).
- ¹³ M. L. Cohen and A. Zettl, *Phys. Today* **63**, 34 (2010).
- ¹⁴ D. Golberg, Y. Bando, Y. Huang, T. Terao, M. Mitome, C. Tang, and C. Zhi, *ACS Nano* **4**, 2979 (2010).
- ¹⁵ A. Nag, K. Raidongia, K. P. S. S. Hembram, R. Datta, U. V. Waghmare, and C. N. R. Rao, *ACS Nano* **4**, 1539 (2010).
- ¹⁶ Y. Shi, C. Hamsen, X. Jia, K. K. Kim, A. Reina, M. Hofmann, A. L. Hsu, K. Zhang, H. Li, Z.-Y. Juang, et al., *Nano Lett.* **10**, 4134 (2010).
- ¹⁷ Y. Lin, T. V. Williams, W. Cao, H. E. Elsayed-Ali, and J. W. Connell, *J. Phys. Chem. C* **114**, 17434 (2010).
- ¹⁸ D. Pacile, J. C. Meyer, Ç. Ö. Girit, and A. Zettl, *Appl. Phys. Lett.* **92**, 133107 (2008).
- ¹⁹ H. Zeng, C. Zhi, Z. Zhang, X. Wei, X. Wang, W. Guo, Y. Bando, and D. Golberg, *Nano Lett.* **10**, 5049 (2010).
- ²⁰ W.-Q. Han, L. Wu, Y. Zhu, K. Watanabe, and T. Taniguchi, *Appl. Phys. Lett.* **93**, 223103 (2008).
- ²¹ C. Zhi, Y. Bando, C. Tang, H. Kuwahara, and D. Golberg, *Adv. Mater.* **21**, 2889 (2009).
- ²² Y. Lin, T. V. Williams, and J. W. Connell, *J. Phys. Chem. Lett.* **1**, 277 (2010).
- ²³ C. Li, Y. Bando, C. Zhi, Y. Huang, and D. Golberg, *Nanotechnology* **20**, 385707 (2009).
- ²⁴ L. Ci, L. Song, C. Jin, D. Jariwala, D. Wu, Y. Li, A. Srivastava, Z. F. Wang, K. Storr, L. Balicas, et al., *Nat. Mater.* **9**, 430 (2010).
- ²⁵ L. Song, L. Ci, H. Lu, P. B. Sorokin, C. Jin, J. Ni, A. G. Kvashnin, D. G. Kvashnin, J. Lou, B. I. Yakobson, et al., *Nano Lett.* **10**, 3209 (2010).
- ²⁶ A. Rubio, J. L. Corkill, and M. L. Cohen, *Phys. Rev. B* **49**, 5081 (1994).
- ²⁷ L. Wirtz, A. Marini, and A. Rubio, *Phys. Rev. Lett.* **96**, 126104 (2006).
- ²⁸ L. Wirtz, A. Rubio, R. A. de la Concha, and A. Loiseau, *Phys. Rev. B* **68**, 045425 (2003).
- ²⁹ M. Topsakal, E. Aktürk, and S. Çıracı, *Phys. Rev. B* **79**, 115442 (2009).

- ³⁰ W.-Q. Han, H.-G. Yu, C. Zhi, J. Wang, Z. Liu, T. Sekiguchi, and Y. Bando, *Nano Lett.* **8**, 491 (2008).
- ³¹ H. Şahin, S. Cahangirov, M. Topsakal, E. Bekaroğlu, E. Aktürk, R. T. Senger, and S. Çıracı, *Phys. Rev. B* **80**, 155453 (2009).
- ³² Z. Zhang and W. Guo, *Phys. Rev. B* **77**, 075403 (2008).
- ³³ C.-H. Park and S. G. Louie, *Nano Lett.* **8**, 2200 (2008).
- ³⁴ L. Liu, T.-K. Sham, W. Han, C. Zhi, and Y. Bando, *ACS Nano* **5**, 631 (2011).
- ³⁵ C.-H. Park, C. D. Spataru, and S. G. Louie, *Phys. Rev. Lett.* **96**, 126105 (2006).
- ³⁶ E. J. Mele and P. Král, *Phys. Rev. Lett.* **88**, 056803 (2002).
- ³⁷ Y. Kubota, K. Watanabe, O. Tsuda, and T. Taniguchi, *Science* **317**, 932 (2007).
- ³⁸ Z.-G. Chen, J. Zou, G. Liu, F. Li, Y. Wang, L. Wang, X.-L. Yuan, T. Sekiguchi, H.-M. Cheng, and G. Q. Lu, *ACS Nano* **2**, 2183 (2008).
- ³⁹ V. Barone and J. E. Peralta, *Nano Lett.* **8**, 2210 (2008).
- ⁴⁰ S. Okada and A. Oshiyama, *Phys. Rev. Lett.* **87**, 146803 (2001).
- ⁴¹ J. Li, G. Zhou, Y. Chen, B.-L. Gu, and W. Duan, *J Am Chem Soc* **131**, 1796 (2009).
- ⁴² D. Golberg, Y. Bando, C. Tang, and C. Zhi, *Adv. Mater.* **19**, 2413 (2007).
- ⁴³ T. Ouyang, Y. Chen, Y. Xie, K. Yang, Z. Bao, and J. Zhong, *Nanotechnology* **21**, 245701 (2010).
- ⁴⁴ I. Savic, D. A. Stewart, and N. Mingo, *Phys. Rev B* **78**, 235434 (2008).
- ⁴⁵ D. A. Stewart, I. Savic, and N. Mingo, *Nano Lett.* **9**, 81 (2009).
- ⁴⁶ C. W. Chang, W. Q. Han, and A. Zettl, *J. Vac Sci & Tech B* **23**, 1883 (2005).
- ⁴⁷ C. W. Chang, A. M. Fennimore, A. Afanasiev, D. Okawa, T. Ikuno, H. Garcia, D. Li, A. Majumdar, and A. Zettl, *Phys. Rev. Lett.* **97**, 085901 (2006).
- ⁴⁸ H. Shen, *Comp. Mater. Sci.* **47**, 220 (2009).
- ⁴⁹ Y. Xiao, X. H. Yan, J. X. Cao, J. W. Ding, Y. L. Mao, and J. Xiang, *Phys. Rev. B* **69**, 205415 (2004).
- ⁵⁰ S. Berber, Y. Kwon, and D. Tomanek, *Phys. Rev. Lett.* **84**, 4613 (2000).
- ⁵¹ D. Donadio and G. Galli, *Phys. Rev. Lett.* **99**, 255502 (2007).
- ⁵² M. Fujii, X. Zhang, H. Xie, H. Ago, K. Takahashi, T. Ikuta, H. Abe, and T. Shimizu, *Phys. Rev. Lett.* **95**, 065502 (2005).
- ⁵³ P. Kim, L. Shi, A. Majumdar, and P. McEuen, *Phys. Rev. Lett.* **87**, 215502 (2001).

- ⁵⁴ N. Mingo and D. A. Broido, Phys. Rev. Lett. **95**, 096105 (2005).
- ⁵⁵ N. Mingo and D. Broido, Nano Lett. **5**, 1221 (2005).
- ⁵⁶ R. S. Prasher, X. J. Hu, Y. Chalopin, N. Mingo, K. Lofgreen, S. Volz, F. Cleri, and P. Koblinski, Phys. Rev. Lett. **102**, 105901 (2009).
- ⁵⁷ J. H. Seol, I. Jo, A. L. Moore, L. Lindsay, Z. H. Aitken, M. T. Pettes, X. Li, Z. Yao, R. Huang, D. Broido, et al., Science **328**, 213 (2010).
- ⁵⁸ A. A. Balandin, S. Ghosh, W. Bao, I. Calizo, D. Teweldebrhan, F. Miao, and C. N. Lau, Nano Lett. **8**, 902 (2008).
- ⁵⁹ S. Ghosh, W. Bao, D. L. Nika, S. Subrina, E. P. Pokatilov, C. N. Lau, and A. A. Balandin, Nat. Mat. **9**, 555 (2010).
- ⁶⁰ W. Cai, A. L. Moore, Y. Zhu, X. Li, S. Chen, L. Shi, and R. S. Ruoff, Nano Lett. **10**, 1645 (2010).
- ⁶¹ C. Faugeras, B. Faugeras, M. Orlita, M. Potemski, R. R. Nair, and A. K. Geim, ACS Nano **4**, 1889 (2010).
- ⁶² W. Li, H. Sevinli, G. Cuniberti, and S. Roche, Phys. Rev. B **82**, 041410 (2010).
- ⁶³ H. Sevinçli and G. Cuniberti, Phys. Rev. B **81**, 113401 (2010).
- ⁶⁴ J. Che, T. Çağın, W. Deng, and W. Goddard III, J. Chem. Phys. **113**, 6888 (2000).
- ⁶⁵ P. K. Schelling, S. R. Phillpot, and P. Koblinski, Phys. Rev. B **65**, 144306 (2002).
- ⁶⁶ B. L. Huang, A. J. H. McGaughey, and M. Kaviany, Int. J. Heat Mass Tran. **50**, 393 (2007).
- ⁶⁷ G. Domingues, S. Volz, K. Joulain, and J. J. Greffet, Phys. Rev. Lett. **94**, 085901 (2005).
- ⁶⁸ L. Lindsay and D. A. Broido, Phys. Rev. B **81**, 205441 (2010).
- ⁶⁹ M. S. Green, J. Chem. Phys. **22**, 398 (1954).
- ⁷⁰ R. Kubo, J. Phys. Soc. Japan **12**, 570 (1957).
- ⁷¹ R. Zwanzig, Annu. Rev. Phys. Chem. **16**, 67 (1965).
- ⁷² M. P. Allen and D. J. Tildesley, *Computer Simulation of Liquids* (Oxford University Press, Oxford, 1987).
- ⁷³ D. A. McQuarrie, *Statistical Mechanics* (University Science Books, California, 2000).
- ⁷⁴ D. C. Rapaport, *The Art of Molecular Dynamics Simulation* (Cambridge University Press, Cambridge, 2004).
- ⁷⁵ M. P. Allen and A. J. Masters, Mol. Phys. **79**, 435 (1993).
- ⁷⁶ J. Haskins, A. Kinaci, and T. Çağın, Nanotechnology **22**, 155701 (2011).

- ⁷⁷ A. Kinaci, J. B. Haskins, and T. Çağın, Submitted to J. Chem. Phys. (????).
- ⁷⁸ J. Tersoff, Phys. Rev. B **39**, 5566 (1989).
- ⁷⁹ G. Kresse and J. Hafner, Phys. Rev. B **47**, 558 (1993).
- ⁸⁰ G. Kresse and J. Furthmüller, Phys. Rev. B **54**, 11169 (1996).
- ⁸¹ R. M. Martin, *Electronic Structure* (Cambridge University Press, Cambridge, England, 2004).
- ⁸² P. E. Blöchl, Phys. Rev. B **50**, 17953 (1994).
- ⁸³ G. Kresse and D. Joubert, Phys. Rev. B **59**, 1758 (1999).
- ⁸⁴ J. P. Perdew, K. Burke, and M. Ernzerhof, Phys. Rev. Lett. **77**, 3865 (1996).
- ⁸⁵ K. Parlinski, Z. Q. Li, and Y. Kawazoe, Phys. Rev. Lett. **78**, 4063 (1997).
- ⁸⁶ P. Carruthers, Rev. Mod. Phys. **33**, 92 (1961).
- ⁸⁷ R. D. Gonçalves, S. Azevedo, F. Moraes, and M. Machado, International Journal of Quantum Chemistry **110**, 1778 (2010).
- ⁸⁸ J. Serrano, A. Bosak, R. Arenal, M. Krisch, K. Watanabe, T. Taniguchi, H. Kanda, A. Rubio, and L. Wirtz, Phys. Rev. Lett. **98**, 095503 (2007).
- ⁸⁹ T. Çağın and J. R. Ray, Phys. Rev. A **37**, 247 (1988).
- ⁹⁰ J. M. Ziman, *Electrons and Phonons* (Oxford University Press, Oxford, 1960).
- ⁹¹ A. Ward and D. A. Broido, Phys. Rev. B **81**, 085205 (2010).
- ⁹² J. E. Turney, E. S. Landry, A. J. H. McGaughey, and C. H. Amon, Phys. Rev. B **79**, 064301 (2009).
- ⁹³ J. Haskins, A. Kinaci, C. Sevik, H. Sevinli, G. Cuniberti, and T. Çağın, ACS Nano **5**, 3779 (2011).
- ⁹⁴ J. W. Evans, L. Hu, and P. Keblinski, Appl. Phys. Lett. **96**, 203112 (2010).
- ⁹⁵ K. Yang, Y. Chen, Y. Xie, X. Wei, T. Ouyang, and J. Zhong, Solid State Communications **151**, 460 (2011).
- ⁹⁶ M. Alaghemandi, E. Algaer, M. C. Böhm, and F. Müller-Plathe, Nanotechnology **20**, 115704 (2009).
- ⁹⁷ G. Zhang and B. Li, The Journal of Chemical Physics **123**, 114714 (2005).
- ⁹⁸ M. A. Osman and D. Srivastava, Nanotechnology **12**, 21 (2001).